Classification of Multicolor Fluorescence *In-Situ* Hybridization (M-FISH) Image Using Structure Based Sparse Representation Model

Jingyao Li, Dongdong Lin, Hongbao Cao
Department of Biomedical Engineering
Tulane University
New Orleans, LA, USA

Yu-Ping Wang
Department of Biomedical Engineering
Tulane University
New Orleans, LA, USA
wyp@tulane.edu

***Abstract*—we developed a structure based sparse representation model for classifying chromosomes in M-FISH images. The sparse representation based classification model used in our previous work only considered one pixel without incorporating any structural information. The new proposed model extends the previous one to multiple pixels case, where each target pixel together with its neighboring pixels will be used simultaneously for classification. We also extend Orthogonal Matching Pursuit (OMP) algorithm to the multiple pixels case, named simultaneous OMP algorithm (SOMP), to solve the structure based sparse representation model. The classification results show that our new model outperforms the previous sparse representation model with the p-value less than 1e-6. We also discussed the effects of several parameters (neighborhood size, sparsity level, and training sample size) on the accuracy of the classification. Our proposed method can be affected by the sparsity level and the neighborhood size but is insensitive to the training sample size. Therefore, the comparison indicates that the structure based sparse representation model can significantly improve the accuracy of the chromosome classification, leading to improved diagnosis of genetic diseases and cancers.**

Keywords- chromosome classification, M-FISH, structure based sparse model

I. INTRODUCTION

Chromosomal rearrangements such as inversions, deletions and translocations result in genetic diseases and cancers. M-FISH is a combinatorial labeling technique used for analyzing these rearrangements [1, 2], which uses 2^N-1 different combinations to distinguish different chromosomes. Human chromosomes include 22 pairs of similar homologous chromosomes and two sex chromosomes (*XY* for male and *XX* for female). Therefore, when *N* equals 5, the binary combinations (presence (1) or absence (0)) of the five fluorophores will be able to distinguish these different types of chromosomes. Figure 1 shows an example of M-FISH images of a male cell. Each image is one channel and the bright areas indicate the presences of chromosomes. The five different color fluorophores are S Gold (F), S Green (G), S Aqua (A), Red (R), S Red (Y) in addition to DAPI (4 in, 6-Diamidino-2-phenylindole) which labels all chromosomes, so in DAPI channel, all chromosomes are visible. Different channels of M-FISH images are acquired by changing the integration time for different color channels. Due to the spectral overlap, uneven intensity level between channels and variations of background surface [3], the analysis of the M-FISH image becomes more challenging in practice, especially in the case for chromosomes.

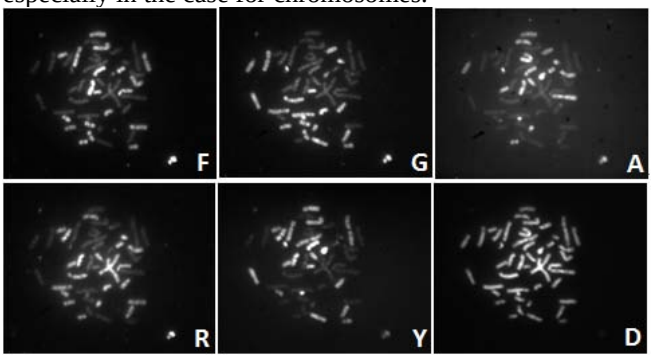

Figure 1. M-FISH images of six different channels

Accurate chromosome classification of M-FISH images is essential for better detection of genetic diseases. To improve the quality of M-FISH images and increase the classification accuracy, many works have been done in the area of preprocessing or post processing methods [3-7]. In classification, some researchers used pixel by pixel classification methods [8-10]，while others used region-based classifiers [6, 7] by considering the relationship of neighboring pixels. We have developed Bayesian [11], adaptive fuzzy c-means (AFCM) method [5] and sparse representations based classification [12]. There have been continuous efforts towards the improvement of the classification for practical use of M-FISH imaging techniques.

In these years there has been an increasing interest in sparse representation in applied mathematics and signal/image processing community because of its advantage of representing high dimensional data [13, 14].

978-1-4673-2560-8/12/$31.00 ©2012 IEEE

Many algorithms including greedy algorithms (Matching Pursuit (MP[15]), OMP[16]), Homotopy [17]and FOCal Underdetermined System Solver (FOCUSS) [18]have been developed to solve the diverse sparse models. Recently sparse approximation from Multiple Measurement Vectors (MMV) has been an area of interest, which jointly recovers a set of vectors that share a common support. MMV problems are common in many applications, such as magnetoencephalography [19], array signal processing [20], cognitive radio and multiband communications [21], and hyperspectral imaging processing [22]. Those applications show that utilizing MMV can greatly improve the analysis results since it can exploit information jointly. Similarly, many algorithms used for solving sparse representation from single measurement vector can be extended to MMV case, *e.g.* M-OMP[18], M-FOCUSS [18] and Second Order Cone Program (SOCP) [23].

In this paper, we developed a new structure based sparse representation model by using MMV for M-FISH classification. The new model extends the often used sparse representation model to the multiple pixels case, where each pixel together with its neighboring pixels will be used simultaneously. The model considers image information of different channels as well as the relationship of neighboring pixels. This model could improve the classification accuracy by utilizing complementary information from different channels and neighboring pixels.

The rest of the paper is organized as follows. In Section Ⅱ the structure based sparse representation model is introduced. In addition, an algorithm SOMP is described to solve the model. In Section Ⅲ the comparison of the model with conventional sparse model on M-FISH image classifications is presented. Section Ⅳ concludes the study.

II. METHOD

Sparse representation has been applied successfully in face recognition [24], hyperspectral imaging classification[22], and M-FISH chromosomal classification in our previous work[12]. In this paper, we introduce a new structure based sparse model for M-FISH chromosomal classification, which takes into account of spatial information of each pixel in the classification.

A. General Sparse Mode

General sparse model is shown in (1). The classifier based on the sparse representation can be designed with matrix $\boldsymbol{A}$ from training data. In classifying hyperspectral images or M-FISH chromosomal images, supposing we have M classes of all pixels and n dimensions for each pixel, matrix $\boldsymbol{A}$ could be divided into M sub-matrices denoted by $\boldsymbol{A} = [\boldsymbol{A}_1, ..., \boldsymbol{A}_i, ..., \boldsymbol{A}_M]$, and A_i can be represented by $\boldsymbol{A_i} = [\boldsymbol{a_1}, \boldsymbol{a_2}, ..., \boldsymbol{a}_{N_i}]$, where each sub-matrix $\boldsymbol{A}_i \in R^{n \times N_i}$ ($N_i > n$). N_i is the number of training samples within the *i*-th class and the total number of pixels used in matrix $\boldsymbol{A}$ is $N = \sum_{i=1}^{M} N_i$. In this work, $\boldsymbol{A}_i$ is obtained by sampling randomly from pixels in the *i*-th chromosome. Each pixel selected from the *i*-th class can be correctly classified by our designed classifier and the solution should be sparse with few non-zero coefficients [12] by the following models.

$$\hat{\boldsymbol{x}} = \min_{\boldsymbol{x}} \|\boldsymbol{A}\boldsymbol{x} - \boldsymbol{y}\|_2 \text{ subject to } \|\boldsymbol{x}\|_p \le K_0 \quad (1)$$

where $\boldsymbol{y} \in R^n$ is a test sample (*i.e.* a pixel) to be classified; $p \in [0,1]$ indicates the norm used to regularize the solution $\hat{\boldsymbol{x}} \in R^N$; K_0 is the parameter used to control the sparsity level of the solution $\hat{\boldsymbol{x}}$. In this work, we discuss the model with $p = 0$, and $\|\boldsymbol{x}\|_0$ is the number of the non-zero entries in the solution $\hat{\boldsymbol{x}}$.

After the design of matrix $\boldsymbol{A}$, for a test pixel $\boldsymbol{y}$ we classify it by the following:

$$Class(\boldsymbol{y}) = \arg\min_{m} \|\boldsymbol{y} - \boldsymbol{A}_m \hat{\boldsymbol{x}}_m\|_2 , m = 1, 2, ..., M \quad (2)$$

The class of $\boldsymbol{y}$ is determined by assigning to the class that best represents the test sample $\boldsymbol{y}$.

B. Structure Based Sparse Model

The general sparse model solves the problem of (1) by considering only one pixel without incorporating any structural information. In many practical scenarios, such as M-FISH image data, each pixel has a strong correlation with its neighboring pixels as shown in Figure 1. In chromosomal region the neighboring pixels usually belong to the same class so the pixels of a chromosome have similar intensity values within a neighbor region. The definition of the neighbor region is the nearest neighborhood of a central pixel, as Figure 2 shows, where y_5 is a central pixel and others are the eight nearest neighboring pixels.

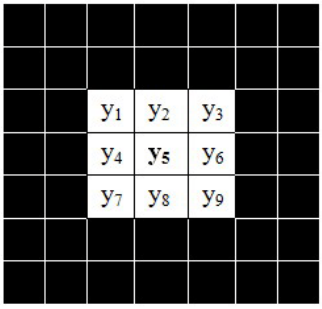

Figure 2. Eight nearest neighboring pixels of a central pixel y5

The spatial relationship among neighboring pixels can be used to significantly improve the classification accuracy and also increase the robustness to the noise. Therefore, we explored a structure based sparse model by considering a region of pixels instead of single pixel in the classification. We extended (1) to the structure based sparse model by computing multiple pixels simultaneously:

$$\hat{\boldsymbol{X}} = \arg\min_{\boldsymbol{X} \in R^{N \times s}} \|\boldsymbol{A}\boldsymbol{X} - \boldsymbol{Y}\|_2 \text{ subject to } \|\boldsymbol{X}\|_{0,q} \le K_0 \quad (3)$$

where $\boldsymbol{Y} = \left[\boldsymbol{y}_1, ... \boldsymbol{y}_j, ... \boldsymbol{y}_s \right]$ contains *s* test pixels with each $\boldsymbol{y}_j$ indicating a single pixel as in (1). These *s* pixels are supposed to be spatially correlated or close. $\boldsymbol{X} = \left[\boldsymbol{x}_1, ... \boldsymbol{x}_j, ... \boldsymbol{x}_s \right]$ is the solution matrix corresponding to the input $\boldsymbol{Y}$. Those solution vectors in $\left\{ \boldsymbol{x}_j \right\}_{j=1,...,s}$ are not independent and have the same non-zeros support, which can be regularized by the term:

$$l_{0,q}: \quad \left\| \boldsymbol{X} \right\|_{0,q} = \left(\sum_i \left\| \boldsymbol{x}^i \right\|_0^q \right)^{1/q} \quad (4)$$

where $\left\| \boldsymbol{X} \right\|_{0,q}$ denotes the number of non-zero rows of $\boldsymbol{X}$, and $\boldsymbol{x}^i$ denotes the *i*-th row of $\boldsymbol{X}$. In this work, we set $q = 2$ .The solution vectors $\left\{ \boldsymbol{x}_j \right\}_{j=1,...,s}$ have the row-wise sparsity, *i.e.*, the non-zeros entries of the solution vectors are in the same rows, which therefore accounts for the correlation of these pixels in the region.

Similar to the classification criteria in (2), after we get $\hat{\boldsymbol{X}}$, (5) is used to identify which class the test sample belongs to,

$$Class(\boldsymbol{Y}) = \arg\min \left\| \boldsymbol{Y} - \boldsymbol{A}_m \hat{\boldsymbol{X}}_m \right\|_2, m = 1, 2, ..., M \quad (5)$$

where $\left\| \boldsymbol{Y} - \boldsymbol{A}_m \hat{\boldsymbol{X}}_m \right\|_2$ is the residual between a test sample $\boldsymbol{Y}$ and the sparse estimation from $\hat{\boldsymbol{X}}_m$.

C. Recovery Algorithm

A variety of algorithms have been proposed to solve the problems of (1) and (3) based on greedy methods. For the general sparse model setting in (1), standard greedy approaches (*i.e. MP*, *OMP*) have been applied to solve the problem with *p*=0[15, 16].In [25], *OMP* was extended to the *MMV* case in (3) as described in Algorithm. The algorithm iteratively chooses an atom $\boldsymbol{a}_k$ from training sample matrix $\boldsymbol{A}$ to best match the current residual matrix by finding the largest *q*-norms of the projection of an atom onto the space spanned by the current residual matrix. The new selected atom is used to re-estimate the signal $\hat{\boldsymbol{X}}_i$ to reduce the residual. The algorithm terminates if the solution has achieved the expected sparsity level K_0 .

Algorithm: Simultaneous Orthogonal Matching Pursuit (SOMP)

Input: training sample matrix $\boldsymbol{A}$, testing sample matrix $\boldsymbol{Y}$

Output: Row-wise sparse matrix $\hat{\boldsymbol{X}}$

Initialization: residual $\boldsymbol{R}_0 = \boldsymbol{Y}$, $\hat{\boldsymbol{X}}_0 = 0$, non-zero rows $\Omega = \varnothing$,*i*=0

while stopping criterion false **do**

1).Find a new atom from matrix $\boldsymbol{A}$ to best approximate the current residual based on *q*-norm: $w = \arg\max_{k \in \Omega} \left\| \boldsymbol{a}_k^T \boldsymbol{R}_{i-1} \right\|_q$

2).Update the non-zero row support $\Omega = \Omega \bigcup \{ w \}$.

3).Update the signal estimation $\hat{\boldsymbol{X}}_i = \left(\boldsymbol{A}_\Omega^T \boldsymbol{A}_\Omega \right)^+ \boldsymbol{A}_\Omega^T \boldsymbol{Y}$, where $\boldsymbol{A}_\Omega$ denotes the sub-matrix of A which is composed of the atoms from matrix $\boldsymbol{A}$, and residual: $\boldsymbol{R}_i = \boldsymbol{Y} - \boldsymbol{A}_\Omega \hat{\boldsymbol{X}}_i$.

4).*i*=*i*+*1*.

end while

Return: $\hat{\boldsymbol{X}} = \hat{\boldsymbol{X}}_i$

III. Result and Analysis

A. M-FISH Database

The comprehensive image database is from Advanced Digital Imaging Research (ADIR; League City, Texas, USA), which is a valuable source for M-FISH studies [18]. In the database each cell contains six channels as shown in Figure 1. In addition, the database includes a ground truth, which is given by an experienced cytogeneticist and can be used to verify the accuracy of the classification. Figure 4(a) shows the ground truth in the form of pseudo color, in which different colors represent different chromosomes. For a male cell the class number is 24, while for a female cell it is 23. The background pixels were labeled by 0, and pixels in the region of overlap were labeled by 255. This data file can be used to validate the accuracy of M-FISH image classification algorithms.

B. Mask Generation

In M-FISH images, most pixels of the image are in background, but we are only interested in the chromosomal region. In order to improve the efficiency of the classifier, DAPI channel was used to generate a mask for the chromosomal region. The AFCM method [5]was employed to get the mask, which was then used for the other five channels. Figure 3 shows a DAPI channel and the mask by the AFCM method.

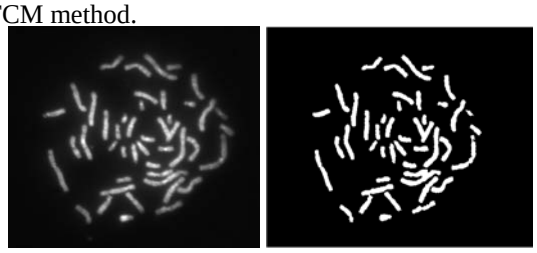

Figure 3. An image of a DAPI channel (left) and the mask generated by the AFCM method (right)

C. M-FISH Training and Testing Data

To train and test the structure based sparse model, 20 cells (10 male, 10 female) were chosen from our data base[26].The training matrix $\boldsymbol{A}$ is composed by sampling pixels in M-FISH images. In each cell, ten training samples were randomly selected from each class. For a male cell, there are 24 different classes, so the size of training sample is 10×24=240. It is 10×23=230 for a female cell. Training matrix $\boldsymbol{A}$ is an *n*×*N* matrix, where *N* denotes the number of training pixels and n denotes the spectral dimension of each

pixel. For the M-FISH images, n equals to 5, because they are 5-channel images. To verify the structure based sparse model, in each cell the rest of the pixels in chromosomal regions were used to test. In (3), the size of testing $\boldsymbol{Y}$ is $n \times s$, where n is the spectral dimension of each pixel, s is the numbers of the neighboring pixels.

D. Classification Results of Different Models

We tested structure based sparse model on M-FISH images and compared the results with previously used sparse model without considering neighboring pixel information. Figure 4(b) and (c) show an example of the comparison of these two models. The Figure 4(b) is the classification results using structure based sparse model, while the Figure 4(c) is the classification results using the sparse model without the structure information. There are more isolated pixels in the chromosomal region in Figure 4(c) than that in Figure 4(b). These isolated pixels are misclassifications without considering structural correlated information within neighboring pixels. Therefore, the structure based sparse model can remove the misclassifications which result from the general sparse model. Figure 5 compares the classification results of two models, in terms of correct classification ratio, which is the ratio of the number of the correct classified pixels to the number of all the pixels in chromosomal region. The red curve is the correct classification ratio using the structure based sparse model while the green one is that of the sparse model without considering structural information. For all 20 cells, the correct classification ratios of structure based sparse model are all greater than those of the previously used sparse model.

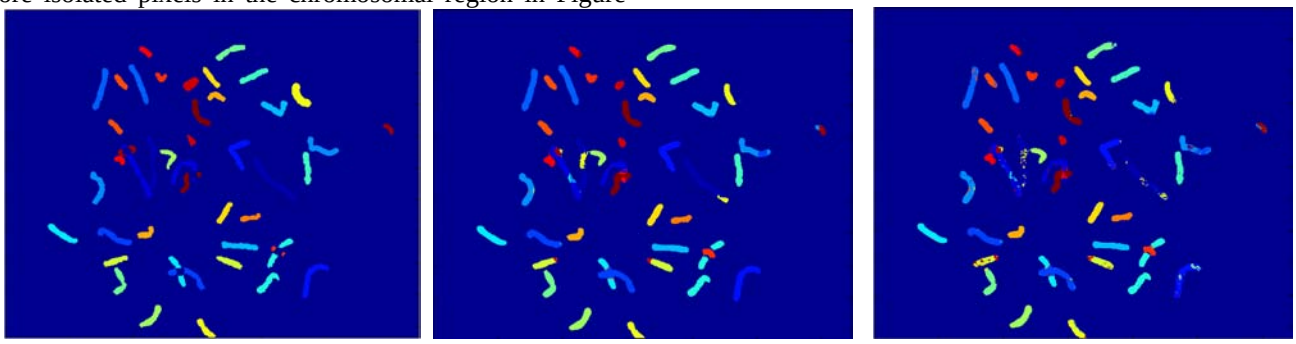

(a) ground truth (b) result of the structure based sparse model (c) result of the sparse model

Figure 4. An example of a ground truth and the results of classification using different models in the form of pseudo color

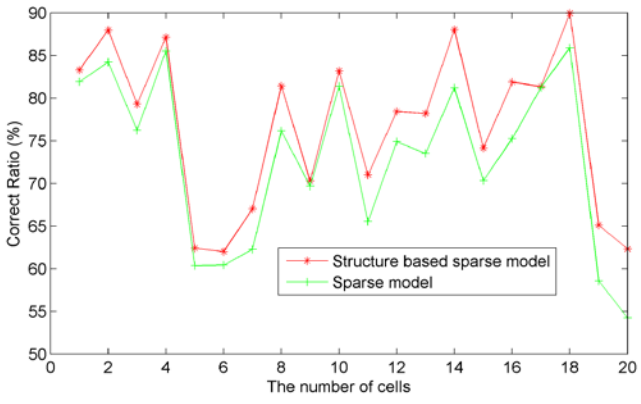

Figure 5. The correct classification ratio using different models

E. Statistical Analysis of Two Models

In order to compare the classification accuracy of these two different models and show the significance of the structure based sparse model, statistical analysis of paired-sample t-test was employed. Figure 6 shows the statistical analysis of the classification accuracy of M-FISH images using different methods. The left one is the box plot of the structure based sparse model, while the right one is that of the sparse model. The structure based sparse model has greater mean value while less standard deviation, 76.72 ± 9.3, than those of the general sparse model which is 72.94 ± 9.82. The p-value of these two models is less than 1e-6 with 95% confidence interval, so the structure based sparse model can significantly improve the accuracy of the chromosomal classification, which in turn improves the ability of M-FISH imaging techniques to diagnose genetic diseases and cancers.

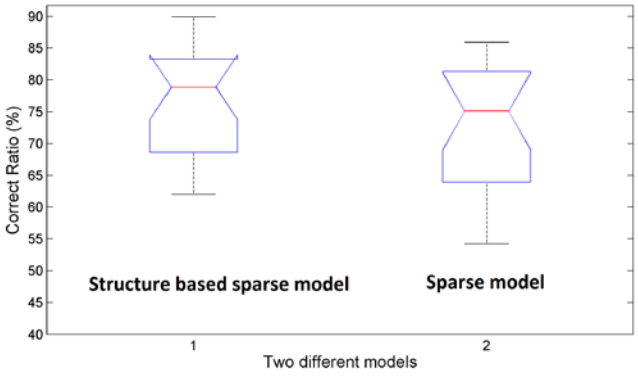

Figure 6. The box plot of classification accuracy using different methods

F. *Parameter Analysis*

The classification accuracy can be affected by adjusting the value of three parameters (neighbor size (*s*), sparsity level (K_0), and training sample size (N_i)). Figure 7 shows the effect of the K_0 and *s* on the correct classification ratios of an M-FISH image. For a fixed K_0, the classification ratio will increase with the increased neighborhood size *s*, but when the neighborhood size is greater than 121, the classification ratio began to decrease. For a fixed neighborhood size *s*, the smaller value of K_0 is, the greater value of the correct classification ratio is.

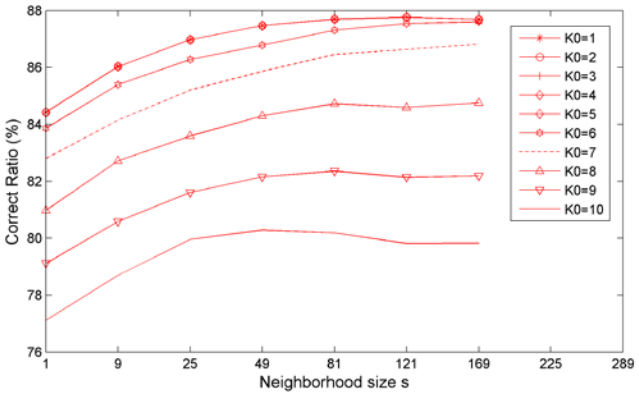

Figure 7. The effect of the K_0 and *s* on the correct classification ratios of an M-FISH image

Next we show the effect of the training sample size on the correct classification ratios in Figure 8. The x axis represents the percentage of training sample in each class. The values of the percentage are 1%, 3%, 5%, 10%, 15%, 20%, 25%, 30%, 35%, 40%, and 50%. The line with stars represents correct classification ratios of the structure based sparse model while the line with triangles represents those of the general sparse model. When the percentage of training samples increases, the correct classification ratios increase in both methods, but these trends are insensitive when the percentage greater than 10%.

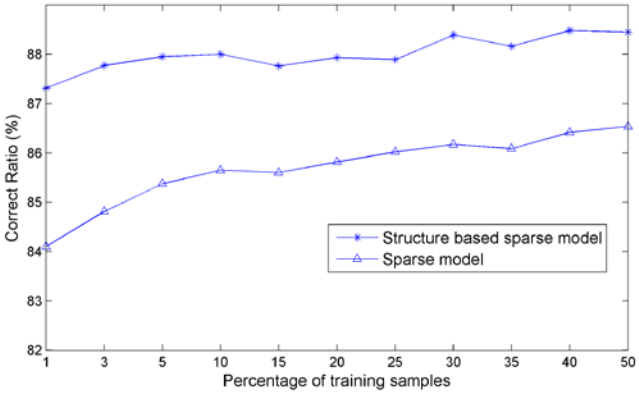

Figure 8. The effect of the different sample sizes on correct classification ratios of an M-FISH image

IV. CONCLLUSION AND DISCUSSION

General sparse model only considers one pixel without imposing any structural information. In this paper we proposed the structure based sparse model which extends the general sparse model to the multiple pixels case, where each pixel together with its neighboring pixels will be used simultaneously for classification. We compared the structure based sparse model with the general sparse model for M-FISH image classification. The statistical analysis shows that the structure sparse model outperforms traditional sparse model, with the p-value less than 1e-6. We also discussed that the effect of parameters of structure based sparse model on the accuracy of the classification. The classification accuracy of our proposed method can be significantly affected by the sparsity level and the neighborhood size but not the training sample size. The comparison indicates that the structure based sparse model can significantly improve the accuracy of the classification, which in turn can better improve the technique to diagnose genetic diseases and cancers.

Although the structure based sparse model can improve the performance of the classifier, the correct classification ratio is still less than 90%. Some preprocessing or post processing steps can be used to further improve the classification accuracy.

REFERENCES

[1] E. Schrock, et al., "Multicolor spectral karyotyping of human chromosomes," Science, vol. 273, pp. 494-497, Jul 26 1996.

[2] M. R. Speicher, et al., "Karyotyping human chromosomes by combinatorial multi-fluor FISH," Nature Genetics, vol. 12, pp. 368-375, Apr 1996.

[3] H. Choi, et al., "Feature normalization via expectation maximization and unsupervised nonparametric classification for M-FISH chromosome images," IEEE Trans Med Imaging, vol. 27, pp. 1107-19, Aug 2008.

[4] H. Choi, et al., "Joint segmentation and classification of M-FISH chromosome images," Conf Proc IEEE Eng Med Biol Soc, vol. 3, pp. 1636-9, 2004.

[5] H. B. Cao, et al., "Segmentation of M-FISH Images for Improved Classification of Chromosomes With an Adaptive Fuzzy C-means Clustering Algorithm," IEEE Transactions on Fuzzy Systems, vol. 20, pp. 1-8, Feb 2012.

[6] P. S. Karvelis, et al., "Enhancement of multichannel chromosome classification using a region-based classifier and vector median filtering," IEEE Trans Inf Technol Biomed, vol. 13, pp. 561-70, Jul 2009.

[7] P. S. Karvelis, et al., "A multichannel watershed-based segmentation method for multispectral chromosome classification," IEEE Trans Med Imaging, vol. 27, pp. 697-708, May 2008.

[8] A. C. B. M. P. Sampat, J. K. Aggarwal, and K. R. Castleman, "Pixel-by-pixel classification of MFISH images," presented at the 24th IEEE Ann. Intern. Conf. (EMBS), Houston, TX, 2002.

[9] W. C. Schwartzkopf, et al., "Maximum-likelihood techniques for joint segmentation-classification of multispectral chromosome images," Ieee Transactions on Medical Imaging, vol. 24, pp. 1593-1610, Dec 2005.

[10] M. P. Sampat, et al., "Supervised parametric and non-parametric classification of chromosome images," Pattern Recognition, vol. 38, pp. 1209-1223, Aug 2005.

[11] Y. P. Wang and K. R. Castleman, "Normalization of multicolor fluorescence in situ hybridization (M-FISH) images for improving color karyotyping," Cytometry Part A, vol. 64A, pp. 101-109, Apr 2005.

[12] H. B. Cao, *et al.*, "Classification of Multicolor Fluorescence In Situ Hybridization (M-FISH) Images With Sparse Representation," IEEETransactions on Nanobioscience, vol. 11, pp. 111-118, Jun 2012.

[13] E. P. Simoncelli and B. A. Olshausen, "Natural image statistics and neural representation," Annu Rev Neurosci, vol. 24, pp. 1193-216, 2001.

[14] Y. Li, et al., "Analysis of sparse representation and blind source separation," Neural Comput, vol. 16, pp. 1193-234, Jun 2004.

[15] S. G. Mallat and Z. F. Zhang, "Matching Pursuits with Time-Frequency Dictionaries," IEEE Transactions on Signal Processing, vol. 41, pp. 3397-3415, Dec 1993.

[16] J. A. Tropp and A. C. Gilbert, "Signal recovery from random measurements via orthogonal matching pursuit," IEEE Transactions on Information Theory, vol. 53, pp. 4655-4666, Dec 2007.

[17] D. L. Donoho and Y. Tsaig, "Fast Solution of l(1)-Norm Minimization Problems When the Solution May Be Sparse," Ieee Transactions on Information Theory, vol. 54, pp. 4789-4812, Nov 2008.

[18] S. F. Cotter, et al., "Sparse solutions to linear inverse problems with multiple measurement vectors," IEEE Transactions on Signal Processing, vol. 53, pp. 2477-2488, Jul 2005.

[19] J. W. Phillips, et al., "MEG-based imaging of focal neuronal current sources," IEEE Trans Med Imaging, vol. 16, pp. 338-48, Jun 1997.

[20] D. Malioutov, et al., "A sparse signal reconstruction perspective for source localization with sensor arrays," IEEE Transactions on Signal Processing, vol. 53, pp. 3010-3022, Aug 2005.

[21] M. Mishali, et al., "Xampling: analog to digital at sub-Nyquist rates," Iet Circuits Devices & Systems, vol. 5, pp. 8-20, Jan 2011.

[22] Y. Chen, et al., "Hyperspectral Image Classification Using Dictionary-Based Sparse Representation," IEEE Transactions on Geoscience and Remote Sensing, vol. 49, pp. 3973-3985, Oct 2011.

[23] Y. C. Eldar and M. Mishali, "Robust Recovery of Signals From a Structured Union of Subspaces," IEEE Transactions on Information Theory, vol. 55, pp. 5302-5316, Nov 2009.

[24] J. Wright, et al., "Robust Face Recognition via Sparse Representation," IEEE Transactions on Pattern Analysis and Machine Intelligence, vol. 31, pp. 210-227, Feb 2009.

[25] J. A. Tropp, et al., "Algorithms for simultaneous sparse approximation. Part I: Greedy pursuit," Signal Processing, vol. 86, pp. 572-588, Mar 2006.

[26] "M-Fish Database website, https://sites.google.com/site/xiaobaocao006/database-for-download.."